

Article

Unique Sequence of Events Triggers Manta Ray Feeding Frenzy in the Southern Great Barrier Reef, Australia

Scarla J. Weeks ^{1,*}, Marites M. Magno-Canto ¹, Fabrice R. A. Jaine ^{1,2}, Jon Brodie ³
and Anthony J. Richardson ^{4,5}

¹ Biophysical Oceanography Group, School of Geography, Planning and Environmental Management, The University of Queensland, St Lucia, QLD 4072, Australia;

E-Mails: m.canto@uq.edu.au (M.M.M.-C.); f.jaine@uq.edu.au (F.R.A.J.)

² Manta Ray and Whale Shark Research Centre, Marine Megafauna Foundation, Praia do Tofo, Inhambane, Mozambique

³ Centre for Tropical Water and Aquatic Ecosystem Research, James Cook University, Townsville, QLD 4811, Australia; E-Mail: jon.brodie@jcu.edu.au

⁴ Oceans and Atmosphere Flagship, CSIRO Marine and Atmospheric Research, EcoSciences Precinct, Dutton Park, Brisbane, QLD 4102, Australia; E-Mail: anthony.richardson@csiro.au

⁵ Centre for Applications in Natural Resource Mathematics (CARM), School of Mathematics and Physics, The University of Queensland, St Lucia, QLD 4072, Australia

* Author to whom correspondence should be addressed; E-Mail: s.weeks@uq.edu.au; Tel.: +61-733-469-056; Fax: +61-733-656-899.

Academic Editors: Raphael M. Kudela and Prasad S. Thenkabail

Received: 16 December 2014 / Accepted: 10 March 2015 / Published: 18 March 2015

Abstract: Manta rays are classified as Vulnerable to Extinction on the IUCN Red List for Threatened Species. In Australia, a key aggregation site for reef manta rays is Lady Elliot Island (LEI) on the Great Barrier Reef, ~7 km from the shelf edge. Here, we investigate the environmental processes that triggered the largest manta ray feeding aggregation yet observed in Australia, in early 2013. We use MODIS sea surface temperature (SST), chlorophyll-*a* concentration and photic depth data, together with *in situ* data, to show that anomalous river discharges led to high chlorophyll (anomalies: 10–15 mg·m⁻³) and turbid (photic depth anomalies: –15 m) river plumes extending out to LEI, and that these became entrained offshore around the periphery of an active cyclonic eddy. Eddy dynamics led to cold bottom intrusions along the shelf edge (6 °C temperature decrease), and at LEI (5 °C temperature decrease). Strongest SST gradients (>1 °C·km⁻¹) were at the convergent frontal

zone between the shelf and eddy-influenced waters, directly overlying LEI. Here, the front intensified on the spring ebb tide to attract and shape the aggregation pattern of foraging manta rays. Future research could focus on mapping the probability and persistence of these ecologically significant frontal zones via remote sensing to aid the management and conservation of marine species.

Keywords: remote sensing; manta rays; frontal zones; sea surface temperature; chlorophyll; photic depth; eddy dynamics; river discharge; upwelling; Great Barrier Reef

1. Introduction

Manta rays are large and highly mobile plankton-feeding elasmobranchs that generally aggregate for limited periods at inshore sites, where they can be readily observed [1,2]. In Eastern Australia, reef manta rays *Manta alfredi* are commonly observed at various locations along the coastline, with some individuals migrating seasonally between sites up to 750 km apart [1,3]. A key aggregation site for reef manta rays is Lady Elliot Island (LEI; 24.1167°S, 152.7167°E) [1,4], a small coral cay at the southernmost limit of the Great Barrier Reef (GBR) and ~7 km from the continental shelf edge (Figure 1 [5]). Here, manta rays are observed year-round, with a peak in occurrence in austral (southern hemisphere) winter (June, July and August) [4]. While the drivers influencing this seasonal variation in abundance are unclear, aggregations of foraging manta rays are commonly observed during austral winter and enhanced food availability has been suggested as a major driver for the austral winter peak in number of manta rays at LEI [4].

As zooplankton is the principal known food resource for manta rays [6], manta foraging can be heavily impacted by environmental processes that influence zooplankton abundance and distribution [7]. Nutrient enrichment via upwelling intrusions is well known to initiate phytoplankton blooms and consequently, large increases in zooplankton [8,9]. Large river discharge events forming river plumes in coastal waters also initiate phytoplankton blooms (and subsequent zooplankton blooms), especially if the rivers have greatly increased nutrient loads from agricultural and urban development on their catchments [10,11]. Stimulation of zooplankton and larval fish populations has been observed at river plume fronts in the GBR [12,13]. River plumes from the Fitzroy River on the southern GBR coast have been documented extending across the shelf to the Capricorn-Bunker Group (Figure 1), following the 1991 large discharge event [14].

The southern GBR region is characterised by the frequent presence of a mesoscale cyclonic eddy, the Capricorn Eddy, which typically forms in the lee of the shelf bathymetry due to variability of the southward-flowing East Australian Current [5]. The eddy can trigger upwelling of cooler, nutrient-enriched oceanic sub-surface waters onto the shelf, transport it to the reef zone and even into the lagoon itself [5,15]. The presence of the eddy has been suggested as an important driver of the seasonal abundance of manta rays at LEI and their distributions within the region [4]. A recent satellite telemetry study [2] has shown that manta rays tagged at LEI preferentially used the eddy, suggesting it as an important foraging ground for the species off Eastern Australia.

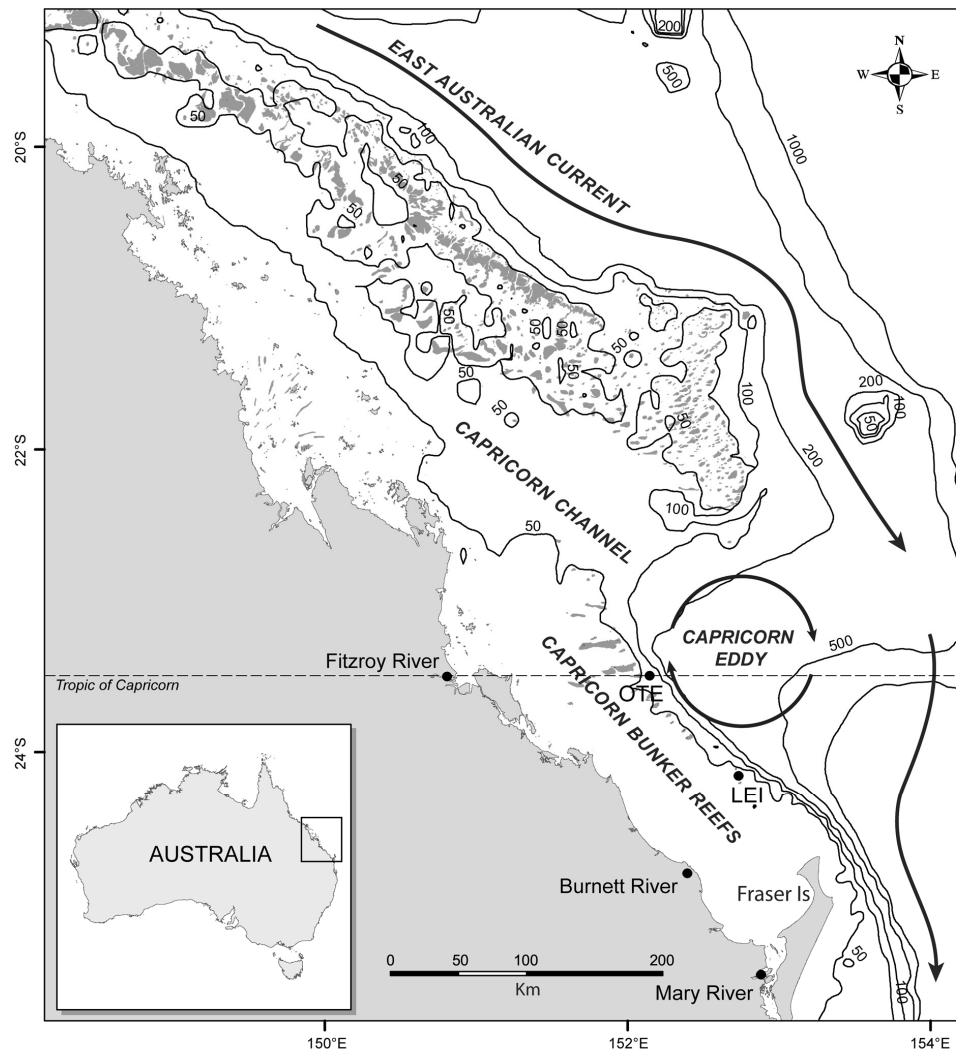


Figure 1. Map of the southern Great Barrier Reef illustrating key bathymetric features, islands and coral reefs, and locations of major river mouths. Dark circular markers close to the shelf edge show the locations of Lady Elliot Island (LEI) and the in-line mooring to the east of One Tree Island (OTE). Modified from [5].

While manta rays can be found all year round at LEI, numbers in austral summer (December, January and February) are typically one-third of those in austral winter [1,4]. Here we report a unique sequence of weather and oceanographic events that triggered a very large aggregation (~150 individuals) of foraging reef manta rays at LEI in the summer of 2013. The primary objectives of this study were: (i) to investigate the environmental processes that led to this anomalous and unseasonal aggregation; and (ii) to determine the potential mesoscale features that could have driven the largest manta ray feeding aggregation yet observed in Eastern Australia.

2. Data and Methods

2.1. Manta Ray Sightings

On two consecutive days at the end of January 2013 (31 January and 1 February), feeding trains of ~150 manta rays were spotted from a small plane approaching the island (Figure 2). All manta rays in

this train were actively foraging, typically swimming underneath the surface, open-mouthed, against the tidal current before turning back and repeating the process in high density prey patches (Kym Fiora *pers. com.*, local dive master). These events were a few days prior to full moon (60%–70% moon illuminated), between 14h00 and 17h00, during the daytime ebb tide. Peak feeding activity was during late ebb flow on 31 January (high tide: 10h40 (2.20 m); low tide: 17h30 (0.45 m)), and similarly on 1 February (high tide: 11h24 (2.09 m); low tide: 17h48 (0.48 m)).

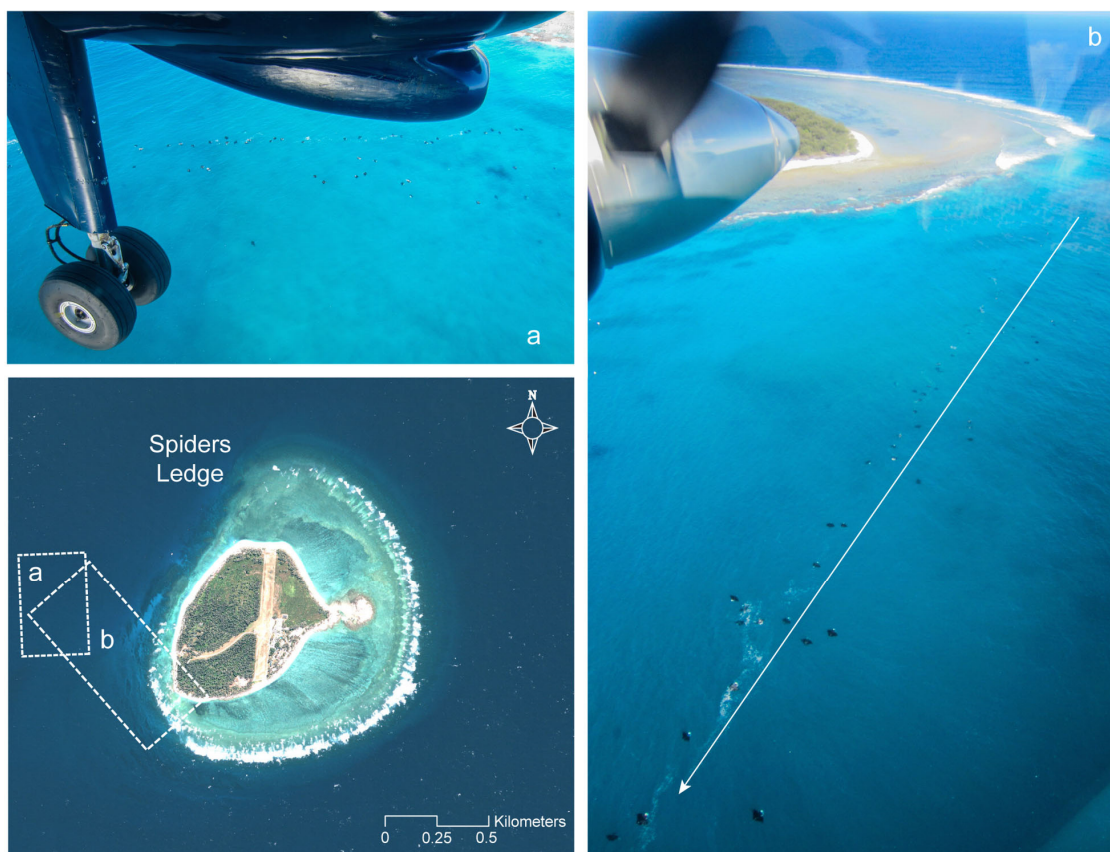


Figure 2. Aerial photographs of the reported manta ray feeding frenzy event on the western side of Lady Elliot Island (LEI) reef on 31 January 2013 at ~16h00. Spatial reference is provided by a Quickbird image of the study area (lower left panel). Dashed white boxes on the Quickbird image show the spatial extent of the associated photographs: (a) approaching LEI; and (b) feeding train of ~150 manta rays. The white arrow in (b) indicates the swimming direction of foraging manta rays. (Photographs courtesy of Bruce and Kate Laverty on Seair Pacific flight to LEI.)

2.2. Weather Conditions

January 2013 was characterised by intense storm activity along the northern to central east coast of Australia as a result of Tropical Cyclone Oswald tracking southwards just inland from the coast. From 22 to 29 January 2013, the storm brought strong winds, high waves and a number of tornadoes, as well as heavy rainfall, particularly along the coast of the southern GBR where rainfall exceeded 400 mm over the last week of January (www.bom.gov.au/climate/current/statements/scs44.pdf). River

discharge data were acquired from the Australian Bureau of Meteorology (www.bom.gov.au/qld/flood) for the Fitzroy, Mary and Burnett Rivers, the primary rivers on the southern GBR coast.

2.3. Satellite Data

Satellite data were derived from the Moderate Resolution Imaging Spectroradiometer (MODIS; modis.gsfc.nasa.gov). To investigate the environmental conditions during the events, time series of daily sea surface temperature (SST), chlorophyll-a concentration (chlorophyll) and photic depth images were generated at 1 km spatial resolution for the period of interest *i.e.*, January and February 2013. To serve as a baseline for comparison, decadal monthly climatologies (2002–2012) were also built at 1 km spatial resolution. Both daytime and night-time data were included in the generation of the SST files. For SST and chlorophyll, standard SST [16] and chlorophyll-a concentration [17] algorithms were used. Algorithms used for estimating chlorophyll concentration are well understood and reliable over deep water, but their applicability in optically shallow regions, such as the GBR, is unclear. However, the strong and obvious features in the mean and anomaly maps present during the event strongly suggest that they are real. Currently, there are efforts to develop an improved algorithm for Case 2 waters of the GBR.

Photic depth data provided a measure of water clarity and was determined by using a GBR-validated photic depth algorithm to establish the depth where 10% of the surface light level is available (GBR $Z_{10\%}$). The methodology is fully described in Weeks *et al.* [18], but in brief: GBR $Z_{10\%}$ was derived by using a quasi-analytical algorithm based on the inherent optical properties of the water column [19,20] and regression of the satellite data against Secchi depth from the GBR. Many of the >5000 records of Secchi depth pre-dated the MODIS-Aqua satellite data (2002–2012), hence both MODIS-Aqua and SeaWiFS data (1997–2010) were used. Satellite to *in situ* “matchups” ($Z_{10\%}$) for the Secchi data were acquired from the NASA Ocean Biology Processing Group (earthdata.nasa.gov/data/data-centers/obpg). Stations in optically shallow water, where the signal is affected by light reflection from the sea floor, were excluded. A Type II linear regression of log-transformed satellite (GBR $Z_{10\%}$) against Secchi values ($Z_{10\%}$) was used:

$$GBR Z_{10\%} = 10^{\left(\frac{\log_{10} Z_{10\%} - a_0}{a_1}\right)} \quad (1)$$

where the slope $a_0 = 0.518$ and the intercept $a_1 = 0.811$ for SeaWiFS data ($r^2 = 0.78$), and $a_0 = 0.529$ and $a_1 = 0.816$ for MODIS-Aqua data ($r^2 = 0.83$). The GBR $Z_{10\%}$ algorithm was implemented in the NASA satellite processing software (SeaDAS; seadas.gsfc.nasa.gov) and applied to the full time series of MODIS-Aqua data. As for SST and chlorophyll, daily photic depth images were generated for the January to February 2013 period of interest and decadal monthly climatologies (2002–2012) built at a 1 km spatial resolution.

To investigate boundaries between different surface water masses, images of frontal gradient intensity were generated. SST and chlorophyll gradients were generated using a SOBEL edge enhancement filter (www.exelisvis.com/docs/SOBEL.html). Prior to edge detection, missing data over small gaps (<3% in total) were filled using a kernel interpolation [21], and a median filter was applied to reduce noise. Pixels over topographic reef features were ignored in the gradient computation.

2.4. In Situ Data

To provide insight into eddy upwelling dynamics along the outer shelf and associated bottom intrusions of waters onto the shelf in the reef zone, *in situ* data were acquired from temperature loggers located near the shelf edge and around the margin of LEI. An in-line mooring located at a depth of 58 m to the east of One Tree Island (OTE), slightly northward of LEI (Figure 1), provided temperature data both near surface (9 m depth) and near the bottom (55 m depth). The OTE mooring is one of a suite deployed by the Australian Integrated Marine Observing System (imos.org.au/661.html) to observe shelf/ocean exchanges along the GBR. Around the margin of LEI, a temperature logger located at a depth of 22 m on ‘Spiders Ledge’ at the northern end of the reef provided near-bottom temperature data at 20.5 m depth. The LEI temperature logger was deployed by Project Manta (ecology.uq.edu.au/content/project-manta-multidisciplinary-study-of-biology-and-ecology-of-iconic-species) in a study to examine drivers of manta ray populations in the region.

Time series of temperature data were generated from the loggers on the OTE mooring for nine months of the austral winter to spring/summer from July 2012 to March 2013. Data were low-pass filtered to remove the tidal signal, following [22]. Temperature data from the Spiders Ledge temperature logger were similarly processed for the 2012/13 austral winter to spring/summer period. To estimate the degree of bottom intrusions onto the shelf and associated stratification of the water column, an upwelling index, defined simply as the temperature difference between the surface and deep layers, was generated for the OTE temperature time series.

3. Results and Discussion

The heavy rainfall along the coast of the southern GBR over the last week of January 2013 led to anomalously high river discharges from the Fitzroy, Mary and Burnett Rivers, with the Burnett River having its highest gauge height in its >130-year record (Figure 3). The total runoff in the 2012–2013 wet season was 23 times higher than the average for the Burnett River and three times higher for the Mary River [23]. These large discharges led to the formation of extensive river plumes intruding onto the southern GBR shelf and phytoplankton blooms with chlorophyll-a concentrations in the range 6–18 mg·m⁻³ [23]. Discharges were enriched with nitrogen and phosphorus from agricultural land use, especially nitrate from fertilizers used in sugarcane cultivation (and other crops) and particulate nitrogen and phosphorus from erosion in beef grazing and cropping lands [24]. Nutrient loads from GBR rivers have increased several-fold over the past 150 years, associated with agricultural development of their catchments [25].

Due to extreme cloud cover during the height of the tropical storm, coincident satellite data over the last week of January 2013 were not useable. As the clouds began to clear, chlorophyll data for early February (Figure 4a) revealed a unique scenario showing not only extremely high chlorophyll waters (a tracer for nutrient-laden river discharge) extending offshore as far as LEI close to the shelf edge, but also the presence of an active Capricorn Eddy in the lee of the shelf bathymetry. Further, it appeared that high chlorophyll shelf waters were being entrained off the shelf, around the periphery of the eddy and re-circulated back towards the shelf by the eddy dynamics. This scenario was similarly apparent in the photic depth data (Figure 4c), with highly turbid inshore waters due to excessive river

discharge extending out to the shelf edge and entrained offshore by the dynamics of the cyclonic eddy. Coincident SST data confirmed the signal of an active Capricorn Eddy in the lee of the shelf bathymetry (Figure 4e). This is despite the satellite sensor measuring surface skin temperature only, which is especially limiting in the subtropical summer when visible surface gradients tend to be masked by a stable and warm surface layer.

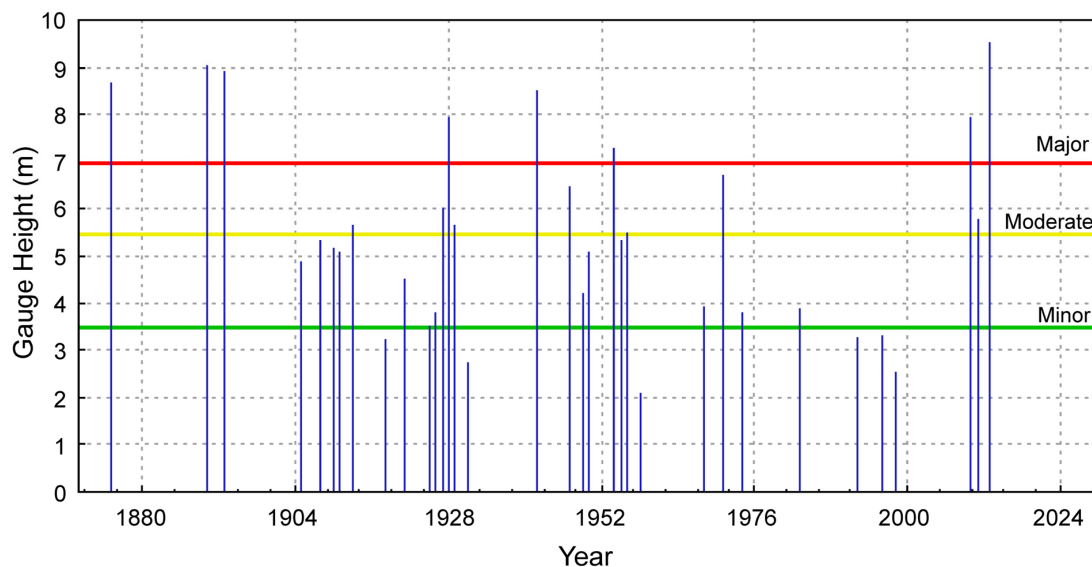


Figure 3. Highest annual flood peaks of the Burnett River on the southern Great Barrier Reef coast showing the 2013 flood led to the highest gauge height in the >130-year record (Generated on 4 April 2013 by the Australian Bureau of Meteorology).

Comparison of the satellite data for early February 2013 with the respective decadal climatologies for February (2002–2012) highlighted the extent of the anomalous conditions: strong positive chlorophyll anomalies ($10\text{--}15\text{ mg}\cdot\text{m}^{-3}$) were seen to extend across the width of the continental shelf in the region (Figure 4b) in accordance with the measured *in situ* chlorophyll-a concentrations [23], with the anomalous off-shelf entrainment and recirculation around the periphery of the eddy clearly apparent. The Capricorn eddy is particularly evident in chlorophyll anomalies expressed in terms of percent change (Appendix). While heavy sediment loads may contaminate the chlorophyll algorithm, the pattern and flow dynamics were confirmed by photic depth values (Figure 4d), determined with the GBR-validated photic depth algorithm [18]. An anomalous decrease in water clarity of up to 15 m as far out as LEI was associated with the cross-shelf extent of river discharge [23,26,27], with similarly turbid shelf waters clearly entrained around the periphery of the eddy. SST anomaly data (Figure 4f) in turn highlighted two opposing bodies of water, with upwelling of cooler, nutrient-enriched oceanic waters by the eddy dynamics manifest even at the surface as an anomalously cool surface expression in the lee of the shelf bathymetry, contrasting with the anomalously warm, turbid shelf waters. Notably, the anomalously cool eddy signal extends onto the shelf beyond the 50 m isobath only at LEI, which lies as a somewhat isolated coral cay, separated from and at the southern limit of the Capricorn Bunker group of reefs (Figure 1).

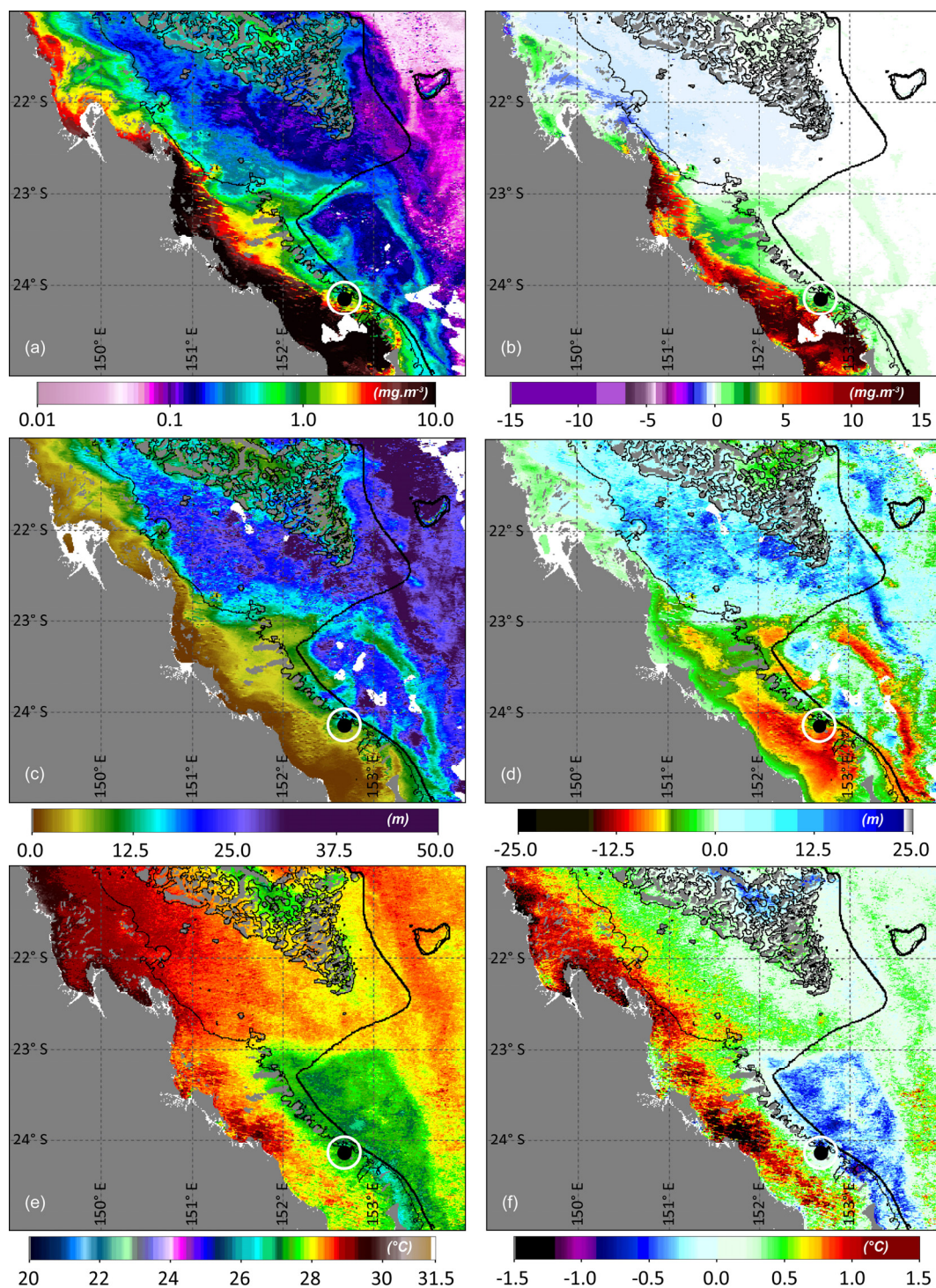


Figure 4. MODIS chlorophyll-*a* ($\text{mg}\cdot\text{m}^{-3}$), photic depth (m) and SST ($^{\circ}\text{C}$) images for the southern GBR (21°S – 25°S ; 149°E – 154°E) for 2 to 4 February 2013. Anomalies are relative to respective February decadal (2002–2012) climatologies. (a) Chlorophyll; (b) chlorophyll anomalies; (c) photic depth; (d) photic depth anomalies; (e) SST and (f) SST anomalies. The black circular marker with white ring shows the location of Lady Elliot Island. The 50 m (thin black) and 200 m (thick black) isobath lines are overlain.

Time series of nine months of temperature data from the loggers on the OTE mooring indicated frequent bottom water temperature fluctuations near the shelf break (Figure 5a). While near surface

temperatures showed a gradual seasonal warming from 21 to 27 °C, temperature observations from deeper in the water column (55 m depth) were interrupted with periods of significant cooling relative to surface waters. At times, the surface water temperature response decouples from that of the cool temperatures deeper in the water column; this increases during periods of cold bottom intrusions where there is enhanced warming of the then stratified shallow surface layer. The most intense and sustained cold bottom intrusions are from mid-January to early February, briefly interrupted (24, 25 January) by strong wind-induced vertical mixing of the water column (Figure 5a) associated with the passing of Tropical Cyclone Oswald. The associated pronounced decrease in bottom temperatures exceeded 6 °C by 2 February, as depicted by the upwelling index (Figure 5b).

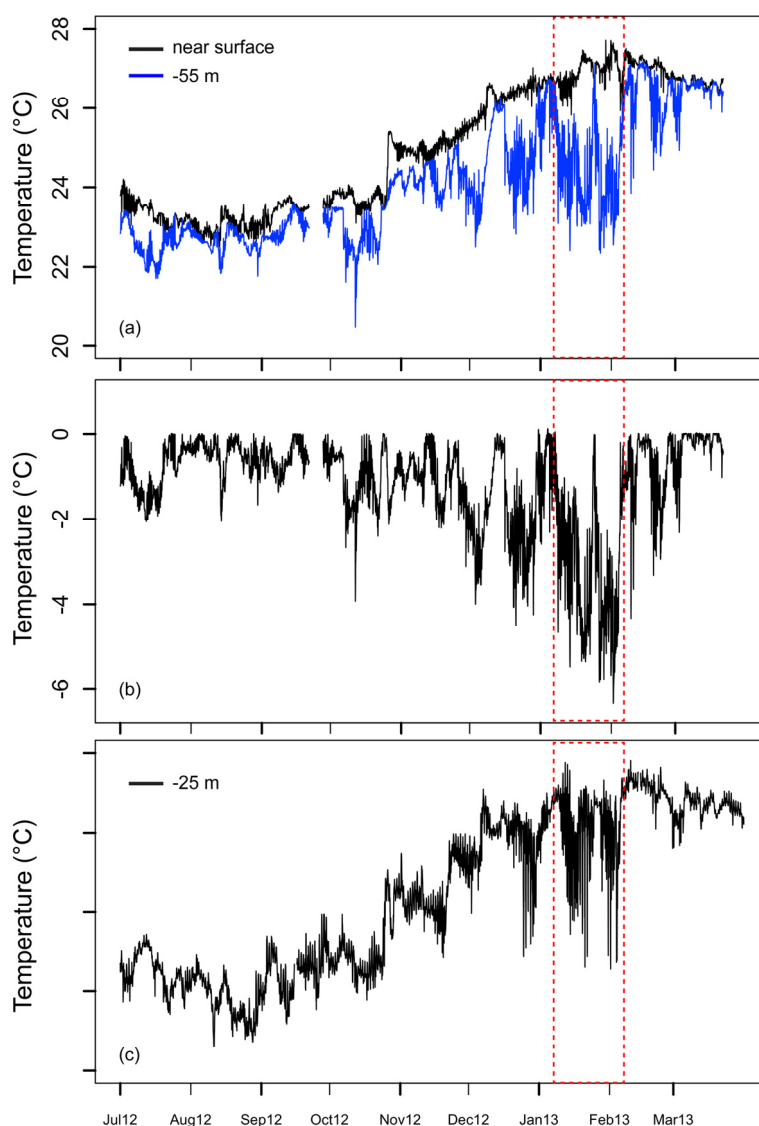


Figure 5. Plots of temperature data from July 2012 to March 2013. **(a)** Concurrent temperature traces from loggers near surface (9 m depth) and near bottom (55 m depth) on an in-line mooring located east of One Tree Island (OTE); **(b)** Upwelling index (temperature difference between 9 m and 55 m depths) for the OTE data; **(c)** Temperature trace from a logger located near bottom (20.5 m depth) on ‘Spiders Ledge’ at Lady Elliot Island. The period from 10 January to 5 February is highlighted by dashed red lines.

This time period is concurrent with the satellite imagery shown in Figure 4 and provides insight into the subsurface processes accompanying the eddy circulation inferred from the remotely sensed data. During periods of enhanced eddy formation, the water column becomes stratified as cool water intrudes onto the shelf. The temperature time series from the Spiders Ledge logger (Figure 5c) clearly shows the presence of the cool bottom water intrusions onto the shelf from mid-January to early February, briefly interrupted by strong cyclone-induced vertical mixing of the water column as at OTE. A drop in near-bottom temperature of up to 5 °C was experienced at LEI, due to intrusions of cool, nutrient-enriched oceanic sub-surface waters onto the shelf.

Ocean Fronts

SST data coincident with the manta ray feeding frenzy clearly revealed SST gradients delineating the periphery of the eddy-influenced surface waters (Figure 6a). However, strongest gradients ($>1 \text{ } ^\circ\text{C}\cdot\text{km}^{-1}$) were at the boundary between the shelf and eddy-influenced waters, and intersecting LEI. The associated chlorophyll data showed strongest chlorophyll gradients related to the cross-shelf extent of nutrient-laden river discharge waters (Figure 6b), with the offshore limit of these similarly coincident with LEI. Moderate chlorophyll gradients also highlighted the boundaries of off-shelf entrained high chlorophyll shelf waters around the periphery of the eddy.

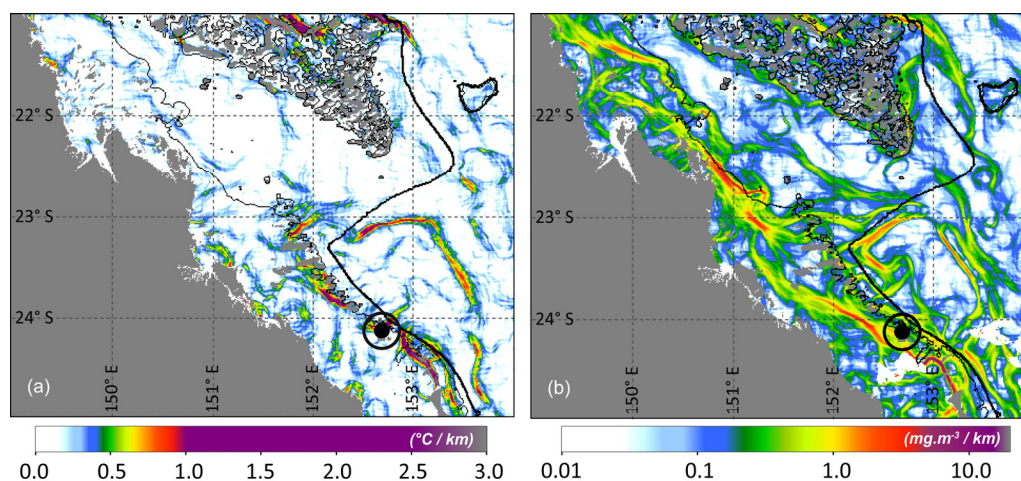


Figure 6. MODIS images of frontal gradient intensity for the southern GBR for 2 to 4 February 2013 showing (a) sea surface temperature gradients; and (b) chlorophyll gradients. The black circular marker with ring shows the location of Lady Elliot Island. The 50 m (thin black) and 200 m (thick black) isobath lines are overlain.

Fronts at the sea surface delineate boundaries between different surface water masses. The dynamic forces involved when two water masses come into proximity act to ensure there is convergence and mixing at their zone of intersection [28]. Tiny, weakly swimming organisms (such as zooplankton) will accumulate at the convergent frontal zone, where the distribution of food particles tends to be highly concentrated, attracting larger nektonic predators [28,29].

Major freshwater input into the ocean tends to provide highly favourable conditions for the development of convergent frontal zones, the runoff producing a lens of less saline, warmer (in summer), less dense surface water relative to more dense oceanic waters. Convergent frontal zones of

contrasting densities resulting from freshwater outflow provide ideal feeding grounds for marine animals [9].

Upwelling and divergence in mesoscale cyclonic eddies lead to convergence near the edges [28]. Remotely sensed thermal and ocean colour fronts mark the interface between cool, nutrient-rich upwelled water and surrounding warmer oligotrophic waters [29]. Eddy dynamics are thus essential to the enrichment, concentration and retention of nutrients and planktonic organisms in surface waters [9], with the peripheries of eddies forming fronts that attract and shape the aggregation patterns of planktivores that prey on the plankton [28,30–32].

Ideally we would have sampled zooplankton during this feeding event, but because it was serendipitous, there was no on-the-ground sampling equipment or personnel. As the event was only about a week after the start of the heavy rainfall, there was likely to be insufficient time for most zooplankton species to increase substantially in numbers [33]. It is thus more likely that the high densities of zooplankton that were likely to be present off LEI and that the manta rays were feeding upon were concentrated by the strong fronts in the region.

In the sequence of events in early 2013, nutrient-laden river waters, with nutrients enriched by nitrogen (nitrate) runoff from fertilizer use in cropping, especially sugarcane cultivation, and particulate nitrogen and phosphorus runoff from erosion in beef grazing lands on the Mary and Burnett Rivers, discharged into the southern GBR lagoon. Both the Burnett and Mary River basins have extensive areas of sugarcane and horticulture cropping and beef grazing lands leading to greatly increased loads of sediment and nutrients [34]. These discharge waters converged on the outer shelf with nutrient-enriched, upwelled oceanic waters intruded onto the shelf via cyclonic eddy dynamics, providing a particularly intense convergent zone in the vicinity of LEI. Tidal flows and reef morphology concentrate zooplankton around island reefs [35–37], and at LEI tidal flows locally concentrate zooplankton biomass on the ebb tide, especially during spring tides [38]. Hence, we conclude that the convergent frontal zone in the vicinity of LEI further intensified on the spring ebb tide to form an intense front that attracted and shaped the aggregation pattern of the observed trains of foraging manta rays aligned along the front.

4. Concluding Remarks

Here we presented an unusual sequence of events of excessive river outflow, dynamic eddy activity, upwelling, convergent fronts and spring ebb tides that together triggered the largest manta ray feeding aggregation yet observed in Eastern Australia. Linking mesoscale oceanographic dynamics to fine-scale events around LEI, we clearly show reef manta rays exploiting an oceanographic front. It should be remembered that although the co-occurrence of high numbers of manta rays and anomalously high chlorophyll is compelling evidence that the oceanographic conditions have led to high densities of zooplankton in the intense fronts, and have attracted large numbers of manta rays to feed, this correlative-type approach does necessarily imply causation. The mechanisms advanced here require validation during future events.

Manta rays are highly mobile plankton-feeding elasmobranchs that are currently listed as Vulnerable to Extinction on the *International Union for Conservation of Nature* (IUCN) Red List for Threatened Species [39]. Oceanic fronts concentrate and retain biological productivity resulting from

nutrient-enrichment processes, attracting and shaping aggregation patterns of planktivores and other species [28,32]. Many marine vertebrates target oceanic fronts for foraging and migration, making frontal zones important sites for conservation [29,40]. Of particular ecological significance in the oceans are persistent mesoscale frontal zones [29,41,42]. Mapping of frontal zones from remotely-sensed data allows identification of the spatio-temporal variability of these ecologically significant foraging habitats, important to dynamic spatial management of our oceans. Future research could focus on mapping the probability and persistence of fronts via remote sensing to aid the management and conservation of marine species in Eastern Australia.

Acknowledgments

We gratefully acknowledge the NASA Ocean Biology Processing Group for provision of MODIS satellite data. We thank Bruce and Kate Laverty for capturing photographs on the Seair Pacific flight to Lady Elliot Island (LEI) and the LEI Eco Resort for continuous support, especially LEI Watersports. Many thanks to Kath Townsend of Project Manta for LEI temperature logger data and Craig Steinberg for providing tidal filter code. *In situ* mooring data were kindly provided by the Integrated Marine Observing System (IMOS)—IMOS is supported by the Australian Government through the National Collaborative Research Infrastructure Strategy and the Super Science Initiative. River flood data were provided by the Australian Bureau of Meteorology.

Author Contributions

Scarla Weeks wrote the manuscript, with input from co-authors. Scarla Weeks, Fabrice Jaine and Anthony Richardson designed the study. Marites Canto wrote the gradient intensity code, generated the satellite images and processed *in situ* data. Jon Brodie provided river discharge data. Marites Canto, Fabrice Jaine and Scarla Weeks produced the figures. Marites Canto and Anthony Richardson addressed the reviewers comments.

Appendix

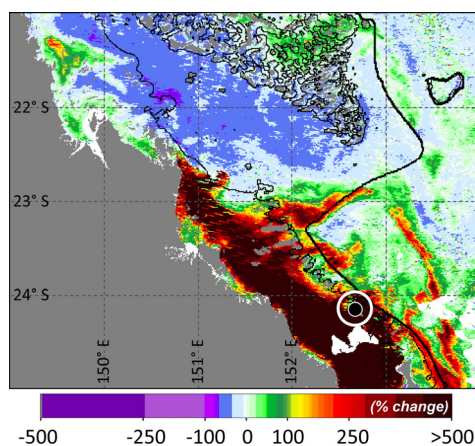


Figure A1. Transformed ($100 \times (\text{Observed} - \text{Climatology})/\text{Climatology}$) MODIS chlorophyll-*a* ($\text{mg}\cdot\text{m}^{-3}$) image for the 2 to 4 February 2013. Climatology inclusive of February decadal period from 2002–2012.

Conflicts of Interest

The authors declare no conflict of interest.

References

1. Couturier, L.I.E.; Jaine, F.R.A.; Townsend, K.A.; Weeks, S.J.; Richardson, A.J.; Bennett, M.B. Distribution, site affinity and regional movements of the Manta Ray, *Manta Alfredi* (krefft, 1868), along the east coast of Australia. *Mar. Freshw. Res.* **2011**, *62*, 628–637.
2. Jaine, F.R.A.; Rohner, C.A.; Weeks, S.J.; Couturier, L.I.E.; Bennett, M.B.; Townsend, K.A.; Richardson, A.J. Movements and habitat use of reef manta rays off eastern Australia: Offshore excursions, deep diving and eddy affinity revealed by satellite telemetry. *Mar. Ecol. Prog. Ser.* **2014**, *510*, 73–86.
3. Couturier, L.I.E.; Dudgeon, C.L.; Pollock, K.H.; Jaine, F.R.A.; Bennett, M.B.; Townsend, K.A.; Weeks, S.J.; Richardson, A.J. Population dynamics of the reef manta ray *Manta alfredi* in eastern Australia. *Coral Reefs* **2014**, *33*, 329–342.
4. Jaine, F.R.A.; Couturier, L.I.E.; Weeks, S.J.; Townsend, K.A.; Bennett, M.B.; Fiora, K.; Richardson, A.J. When giants turn up: Sighting trends, environmental influences and habitat use of the manta ray *Manta alfredi* at a coral reef. *PLoS One* **2012**, *7*, e46170.
5. Weeks, S.; Bakun, A.; Steinberg, C.; Brinkman, R.; Hoegh-Guldberg, O. The Capricorn Eddy: A prominent driver of the ecology and future of the southern Great Barrier Reef. *Coral Reefs* **2010**, *29*, 975–985.
6. Couturier, L.I.E.; Rohner, C.A.; Richardson, A.J.; Marshall, A.D.; Jaine, F.R.A.; Bennett, M.B.; Townsend, K.A.; Weeks, S.J.; Nichols, P.D. Stable isotope and signature fatty acid analyses suggest reef manta rays feed on demersal zooplankton. *PLoS One* **2013**, *8*, e77152.
7. Richardson, A.J. In hot water: Zooplankton and climate change. *ICES J. Mar. Sci.* **2008**, *65*, 279–295.
8. Andrews, J.C.; Gentien, P. Upwelling as a source of nutrients for the great barrier reef ecosystems: A solution to darwin's question? *Mar. Ecol. Prog. Ser.* **1982**, *8*, 257–269.
9. Bakun, A. *Patterns in the Ocean: Ocean Processes and Marine Population Dynamics*; University of California Sea Grant: San Diego, CA, USA, 1996; p. 323.
10. Dagg, M.; Benner, R.; Lohrenz, S.; Lawrence, D. Transformation of dissolved and particulate materials on continental shelves influenced by large rivers: Plume processes. *Cont. Shelf Res.* **2004**, *24*, 833–858.
11. Brodie, J.; Schroeder, T.; Rohde, K.; Faithful, J.; Masters, B.; Dekker, A.; Brando, V.; Maughan, M. Dispersal of suspended sediments and nutrients in the Great Barrier Reef lagoon during river-discharge events: Conclusions from satellite remote sensing and concurrent flood-plume sampling. *Mar. Freshw. Res.* **2010**, *61*, 651–664.
12. McKinnon, A.D.; Thorrold, S.R. Zooplankton community structure and copepod egg production in coastal waters of the central Great Barrier Reef lagoon. *J. Plankton Res.* **1993**, *15*, 1387–1411.
13. Thorrold, S.R.; McKinnon, A.D. Responses of larval assemblages to a riverine plume in coastal waters of the central Great Barrier Reef. *Limnol. Oceanogr.* **1995**, *40*, 177–181.

14. Devlin, M.J.; Brodie, J. Terrestrial discharge into the Great Barrier Reef lagoon: Nutrient behavior in coastal waters. *Mar. Pollut. Bull.* **2005**, *51*, 9–22.
15. Kleypas, J.A.; Burrage, D.M. Satellite observations of circulation in the southern Great Barrier Reef, Australia. *Int. J. Remote Sens.* **1994**, *15*, 2051–2063.
16. Brown, O.B.; Minnett, P.J. *MODIS Infrared Sea Surface Temperature Algorithm, Algorithm Theoretical Basis Document, v2.0*; University of Miami: Miami, FL, USA, 1999.
17. O'Reilly, J.E.; Coauthors, A. *SeaWiFS Postlaunch Calibration and Validation Analyses, Part 3*; NASA Goddard Space Flight Center, NASA: Washington, DC, USA, 2000; p. 49.
18. Weeks, S.; Werdell, P.J.; Schaffelke, B.; Canto, M.; Lee, Z.; Wilding, J.G.; Feldman, G.C. Satellite-derived photic depth on the Great Barrier Reef: Spatio-temporal patterns of water clarity. *Remote Sens.* **2012**, *4*, 3781–3795.
19. Lee, Z.; Carder, K.L.; Arnone, R.A. Deriving inherent optical properties from water color: A multiband quasi-analytical algorithm for optically deep waters. *Appl. Opt.* **2002**, *41*, 5755–5772.
20. Lee, Z.P.; Weidemann, A.; Kindle, J.; Arnone, R.; Carder, K.L.; Davis, C. Euphotic zone depth: Its derivation and implication to ocean-color remote sensing. *Geophys. Res.* **2007**, *112*, 1–11.
21. Mühlenstädt, T.; Kuhnert, S. Kernel interpolation. *Comput. Stat. Data Anal.* **2011**, *55*, 2962–2974.
22. Thompson, R.O.R.Y. Low-pass filters to suppress inertial and tidal frequencies. *J. Phys. Oceanogr.* **1983**, *13*, 1077–1083.
23. Da Silva, E.T.; Devlin, M.; Wenger, A.; Petus, C. *Burnett-Mary Wet Season 2012–2013: Water Quality Data Sampling, Analysis and Comparison against Wet Season 2010–2011 Data*; James Cook University: Townsville, QLD, Australia, 2013; p. 31.
24. Waterhouse, J.; Brodie, J.; Lewis, S.; Mitchell, A. Quantifying the sources of pollutants in the Great Barrier Reef catchments and the relative risk to reef ecosystems. *Mar. Pollut. Bull.* **2012**, *65*, 394–406.
25. Kroon, F.J.; Kuhnert, P.M.; Henderson, B.L.; Wilkinson, S.N.; Kinsey-Henderson, A.; Abbott, B.; Brodie, J.E.; Turner, R.D.R. River loads of suspended solids, nitrogen, phosphorus and herbicides delivered to the Great Barrier Reef lagoon. *Mar. Pollut. Bull.* **2012**, *65*, 167–181.
26. Fabricius, K.E.; Logan, M.; Weeks, S.; Brodie, J. The effects of river run-off on water clarity across the central Great Barrier Reef. *Mar. Pollut. Bull.* **2014**, *84*, 191–200.
27. Alvarez-Romero, J.G.; Devlin, M.; Da Silva, E.T.; Petus, C.; Ban, N.C.; Pressey, R.L.; Kool, J.; Roberts, J.J.; Cerdeira-Estrada, S.; Wenger, A.S.; *et al.* A novel approach to model exposure of coastal-marine ecosystems to riverine flood plumes based on remote sensing techniques. *J. Environ. Manag.* **2013**, *119*, 194–207.
28. Bakun, A. Fronts and eddies as key structures in the habitat of marine fish larvae: Opportunity, adaptive response and competitive advantage. *Sci. Mar.* **2006**, *70*, 105–122.
29. Scales, K.L.; Miller, P.I.; Hawkes, L.A.; Ingram, S.N.; Sims, D.W.; Votier, S.C. On the front line: Frontal zones as priority at-sea conservation areas for mobile marine vertebrates. *J. Appl. Ecol.* **2014**, *51*, 1575–1583.
30. Bertrand, A.; Gerlotto, F.; Bertrand, S.; Gutierrez, M.; Alza, L.; Chipollini, A.; Diaz, E.; Espinoza, P.; Ledesma, J.; Quesquen, R.; *et al.* Schooling behaviour and environmental forcing in relation to anchoveta distribution: An analysis across multiple spatial scales. *Prog. Oceanogr.* **2008**, *79*, 264–277.

31. Sabarros, P.; Ménard, F.; Lévênez, J.; Tew-Kai, E.; Ternon, J. Mesoscale eddies influence distribution and aggregation patterns of micronekton in the Mozambique Channel. *Mar. Ecol. Prog. Ser.* **2009**, *395*, 101–107.
32. Godo, O.R.; Samuelsen, A.; Macaulay, G.J.; Patel, R.; Hjollo, S.S.; Horne, J.; Kaartvedt, S.; Johannessen, J.A. Mesoscale eddies are oases for higher trophic marine life. *PLoS One* **2012**, *7*, 1–9.
33. Richardson, A.J.; Verheye, H.M. The relative importance of food and temperature to copepod egg production and somatic growth in the southern Benguela upwelling system. *J. Plankton Res.* **1998**, *20*, 2379–2399.
34. Brodie, J.E.; Kroon, F.J.; Schaffelke, B.; Wolanski, E.C.; Lewis, S.E.; Devlin, M.J.; Bohnet, I.C.; Bainbridge, Z.T.; Waterhouse, J.; Davis, A.M. Terrestrial pollutant runoff to the Great Barrier Reef: An update of issues, priorities and management responses. *Mar. Pollut. Bull.* **2012**, *65*, 81–100.
35. Estrade, P.; Middleton, J.H. A numerical study of island wake generated by an elliptical tidal flow. *Cont. Shelf Res.* **2010**, *30*, 1120–1135.
36. O'Shea, O.R.; Kingsford, M.J.; Seymour, J. Tide-related periodicity of manta rays and sharks to cleaning stations on a coral reef. *Mar. Freshw. Res.* **2010**, *61*, 65–73.
37. Andrade, I.; Sangrà, P.; Hormazabal, S.; Correa-Ramirez, M. Island mass effect in the Juan Fernández archipelago (33° S), Southeastern Pacific. *Deep Sea Res. I Oceanogr. Res. Pap.* **2014**, *84*, 86–99.
38. Armstrong, A. *Where can I Find a Decent Meal? Foraging Conditions at an Aggregation Site for Reef Manta Rays on the Great Barrier Reef*; University of Queensland: Brisbane, Australia, 2014.
39. Marshall, A.D.; Bennett, M.B. The frequency and effect of shark-inflicted bite injuries to the reef manta ray *Manta alfredi*. *Afr. J. Mar. Sci.* **2010**, *32*, 573–580.
40. Miller, P.I.; Christodoulou, S. Frequent locations of oceanic fronts as an indicator of pelagic diversity: Application to marine protected areas and renewables. *Mar. Policy* **2013**, *45*, 318–329.
41. Polovina, J.J.; Howell, E.; Kobayashi, D.R.; Seki, M.P. The transition zone chlorophyll front, a dynamic global feature defining migration and forage habitat for marine resources. *Prog. Oceanogr.* **2001**, *49*, 469–483.
42. Bost, C.A.; Cotté, C.; Bailleul, F.; Cherel, Y.; Charrassin, J.B.; Guinet, C.; Ainley, D.G.; Weimerskirch, H. The importance of oceanographic fronts to marine birds and mammals of the Southern Oceans. *J. Mar. Syst.* **2009**, *78*, 363–376.